Colour and ultrasound propagation speed changes by different ageing of freezing/thawing and cooling/heating in granitic materials

A. C. Iñigo[a*], J. García-Talegón[b], S. Vicente-Tavera[c], S. Martín-González[a], S. Casado-Marín[a], M. Vargas-Muñoz[d], J. L. Pérez-Rodríguez[d]

[a]Instituto de Recursos Naturales y Agrobiología de Salamanca (IRNASA-CSIC), Spain.

[b]Departamento de Geología, Universidad de Salamanca, Spain.

[c]Departamento de Estadística, Universidad de Salamanca, Spain.

[d]Instituto de Ciencias de Materiales de Sevilla (ICMSE-CSIC), Spain.

[*]Correspondence to: A. C. Iñigo, Instituto de Recursos Naturales y Agrobiología de Salamanca (IRNASA-CSIC), c) Cordel de Merinas 40-52, 37008 Salamanca. Tel.: (+) 34 923 219606. Fax: (+) 34 923 219609. E-mail: adolfo.inigo@irnasa.csic.es

Abstract

In the present work we determined the chromatic coordinates (L*,a*,b*) and ultrasound propagation speeds on the three spatial planes (V_x,V_y,V_z) of three ornamental granites (Aqueduct of Segovia, Spain) before, during, and after being subjected to 70 cycles of two types of accelerated ageing (typical of cold regions): a) freezing/thawing and cooling/heating (T1), and b) freezing/thawing and cooling/heating + salt crystallization (T2). A multivariate technique (Canonical Biplot) was applied to the data obtained, with the observation of significant variations between the two types of accelerated artificial ageing as compared with those obtained in quarry rock in the three chromatic

coordinates (L*,a*,b*). With regard to the ultrasound propagation speed, we only detected differences in the results of the T2 artificial ageing treatment with respect to those of quarry rock. This fact is confirmed by the estimated data of resistance to compression.

Key words: Freezing/thawing, Granitic rocks**,** Weathering**,** Colour, Ultrasound propagation speed, Canonical Biplot.

1 Introduction

In Segovia, located in the Regional Community of Castilla y León (Spain), with a Mediterranean climate with a continental trend [cold region, characterized by sharp and sudden thermal oscillation (up to as much as 40ºC between the day and the night) give rise to the so-called thermoclastic phenomena and weathering through freezing appears in humid areas, where the temperature is fairly low. Where permanent humidity exists, weathering is also produced by precipitation and crystallization of salts in pores], the mechanisms that have most frequently given rise to degradation due to climate are as follows (García-Talegón et al., 2006a, 2006b; Iñigo et al., 2000a, 2003; Rives and García-Talegón, 2006; Vicente, 1996):

a) Freezing/thawing and cooling/heating (T1)

b) Freezing/thawing and cooling/heating + salt crystallization (T2)

These methods of artificial ageing were used under controlled conditions in a simulation chamber.

Extreme changes in temperature cause differential expansion between mineral grains in granitic materials. These expansions generate micro-discontinuities, allowing the circulation of fluids (water, dissolved salts, etc.) (Takarli et al., 2008). The fluids react in the rock-fluid interface, producing solutions and/or precipitation reactions (Sausse et al., 2001).

When water freezes, it produces a volume increase generating micropores (about 9% of original volume). This expansion induces stress concentration and tensile damage in micropores (Iñigo et al., 2000b). When the rock thaws, the water flows through the micropores causing new fractures (Matsuoka,1990, Hori and Morihiro, 1998; Chen et al., 2004; Tan et al., 2011).

The properties of the granites (initial porosity, the pore size distribution and mineral content) have a great influence on deterioration (Iñigo et al., 2000). These authors used the nitrogen adsorption technique to study the specific surface area and the pore size distribution of five types of granites. This method allows detection of pores with a diameter <1 μm. It is well known that pores in this diameter range play an important role in degradation processes such as haloclasty and gelifraction (Camuffo, 1996).

Colour is a parameter that must be currently controlled to monitor the quality a quarry rock when it is used in a monument, both as regards its deterioration due to environmental (Sebastián-Pardo and Zezza, 1998; Zezza, 2002a) and microenvironmental factors in certain zones of buildings (Zezza, 2002b) and after the application of conservation treatments (García-Talegón et al., 1998; Iñigo et al., 1997, 2004).

Additionally, another important variable to be controlled both in ageing and in the application of conservation treatments is measurement of the ultrasound propagation speed, which for example indicates a decrease of cohesion of minerals as a result of T1 an T2 ageing (Chen et al., 2004 and Matsuoka, 1990), or an increase in this parameter due to application of a conservation treatment (consolidation).

The main objective of this work was to investigate the influence of freeze–thaw cycles, with (T2) or without (T1) the presence of salts in water (sulphates), on the chromatic coordinates (L*,a*,b*) and ultrasound propagation speeds on the three spatial axes (V_x,V_y,V_z). This variations in the colour and ultrasound propagation speeds were studied applying a multivariate method (Canonical Biplot) to the data obtained concerning these variables to 3 of the granites most widely used in the construction and successive

interventions of the Roman Aqueduct in Segovia (Ortigosa del Monte, La Granja and Magullo) before, during, and after subjection to 70 cycles of the two types of ageing used. Additionally, we determined possible weight losses by ANOVA analysis after the application of the two types of ageing applied in the controlled cycle. We propose also a linear regression model between the resistance to compression and the ultrasonic propagation speed in granites.

2 Materials and methods

The granite materials most used in construction and later interventions on the aqueduct in Segovia are from Ortigosa del Monte, La Granja, and Magullo. Their mineralogical composition was determined by X-ray diffraction. As expected, the main minerals were quartz (Q), potassium feldspars (Fk), plagioclase (Pl) and micas (I/M), Table 1.

Using the results of the chemical analysis of the major elements (Table 2), we classified the three varieties according to the CIPW normative calculation (Q'-ANOR') (Streckeisen and Le Maitre, 1979), observing that the Ortigosa del Monte material corresponded to a sienogranite; that from La Granja to a monzogranite, and that from Magullo to a granodiorite, Fig. 1. This classification confirms the microscopy observations. Magullo was the variety with the most calcic plagioclases (anorthite) and the Ortigosa del Monte material had the most sodic plagioclases.

The stones were cut in cubic samples (5 x 5 x 5 cm), and were subjected to 70 cycles of the following accelerated ageing treatments in a simulation chamber under controlled conditions:

T1: Freezing/thawing and cooling/heating (-20 to 110°C). After a drying period at 60 ºC until constant weight was reached, the blocks were submerged in distilled water for 16 hours (rocks are saturated), after which they were cooled to -20ºC and kept at that temperature for 3 hours. Following this, temperature was raised to 110ºC (rate = 2ºC/min), and the blocks were held at that temperature for 3 hours. Finally, the blocks were left for 2 hours at room temperature and the process was started again (Tiano and Pecchioni, 1990 and Iñigo et al., 2000a).

T2: The experiment was carried out over a combined freezing/thawing and cooling/heating treatment with sulphate crystallization. We used the method T1, but the samples are immersed in a 14% solution of hydrated sodium sulphate ($Na_2SO_4 \cdot 10H_2O$) instead of distilled water.

The chromatic coordinates (L*,a*,b*) were measured with a MINOLTA model CR-310 colorimeter for solids during cycles 0 (before starting each of the artificial ageing treatments) 20, 40, 60 and 70.

Ultrasound speed was measured in the same number of cycles as colour during the ageing treatments. To accomplish this, an ULTRASONIIC Tester BP-5 from STEINKAMP was used.

To study the influence of the number of ageing cycles (freezing/thawing and cooling/heating, and freezing/thawing and cooling/heating + salt crystallization) on the quarry samples, the multivariate technique known as Canonical Biplot (Varas et al., 2005 and Amaro et al., 2008) was used.

The Canonical Biplot is equivalent to MANOVA analysis (Multivariate Analysis of Variance), but it includes all the characteristics of the Biplot method (Gabriel, 1971, 1972, 1995), which is aimed at discriminating the set of groups of previously

established populations. This technique was later developed and completed (Amaro, 2004; Galindo, 1986; Vicente-Villardón, 2012), and applied to the field of cultural heritage conservation (Iñigo et al., 2004; Varas et al., 2005; Vicente and Vicente-Tavera, 2001).

The results are summarized on several factor planes, where the variables are represented as vectors that start out from a hypothetical origin and the means of the different groups as stars surrounded by confidence circles in the same reference system. If two variables are represented with a very small angle then the variables are highly correlated: if they are opposite their correlation is inverse. Additionally, if the angle is close to perpendicularity, their correlation is minimum. On projecting all the star markers perpendicularly onto the directions of any of the variables, the order of the projections in the direction of those variables is equivalent to the value that the population means take on that variable. If two confidence circles are projected perpendicularly on one of the variables and the intervals of both projections do not overlap, this is tantamount to saying that there are differences between both means (Students' t test); the amplitudes of the circles will depend on the significance, α, determined (MSD, Bonferroni corrections, etc.). These interpretations are subject to a series of measurements of the quality of representation for the different planes (inertia absorption of the planes, the goodness of the projections of the measurements on the variables for the dimensions selected, etc.).

In our case, we started out from a matrix formed by 900 rows and 6 columns (variables). The rows were divided into 27 groups (populations) with specific characteristics:

Varieties of granite (V): Ortigosa del Monte (O), La Granja (G) and Magullo (M).

Types of ageing (T): freezing/thawing and cooling/heating (TI) and freezing/thawing and cooling/heating + salt crystallization. (T2).

Number of cycles (C): 0, 20, 40, 60 and 70.

The denomination of the populations shown in the figures is of the VTC type. Thus, for example, a population of samples from G that was subjected to 40 ageing cycles with freezing/thawing and cooling/heating would be known as GT140. This type of combination affords 24 different populations. The remaining three correspond the quarry varieties not aged (ORT00, GRA00 and MAG00).

The variables studied refer to the different chromatic coordinates (L*,a*,b*) and the ultrasound propagation speeds defined on the three axes of coordinates (V_x,V_y,V_z).

This technique provides a global contrast (like the classic MANOVA), called the Wilk's lambda.

On the plane 1-2, Fig. 2, we have the simultaneous groups and variables representation. We differentiated the types of ageing (T1 and T2) by discontinuous and continuous lines respectively, representing each variety on plane 1-2, Fig. 2, in three differentiated figures (Figs. 3, 4 and 5) in order to better see the possible differences and magnitudes of the effects among the groups. In these last three figures (Figs. 3, 4 and 5) only represent the confidence circles and labels of the type of granite markers analyzed (La Granja, Magullo and Ortigosa del Monte respectively).

Table 3 shows the means and Standard errors (S.E.) of the variables studied (colour coordinates and the ultrasound speed) of different varieties of granite.

The study of the resistance to compression (mechanical property) was performed with similar granites from Avila (Spain), Porto and Braga (Portugal), altered or no in

quarry, Table 4. We use a linear regression model, where the dependent variable is resistance to compression (RC; it is the maximum load per unit area that is capable of supporting a specimen up to failure; UNE, 1985) and average of ultrasound propagation speed as independent [$V=(V_x + V_y + V_z)/3$]. We have included a dumy variable (altered, 0 = not altered and 1 = altered). The linear correlation coefficient is $r = 0.765$ ($p<0.01$).

The linear regression model was:

$$RC = 146.983 + 0.203 \times V - 153.971 \text{ Altered (0 = not altered and 1 = altered)}$$

where:

RC = Resistance to compression (Kg/cm^2)

V = Average of ultrasound propagation speed (m/s)

Table 5 shows the linear correlation coefficient (r) and coefficient of determination or goodness of fit (R^2). ANOVA table of the model ($p<0.01$) and model coefficients ($\beta_0 = 146.983$, $p>0.05$; $\beta_1 = 0.203$, $p<0.01$ and $\beta_2 = -153.971$, $p>0.05$). We can observe that increasing a unit in V, RC increases 0.203 units. Also, we can see how the RC is less than 153.971 units in altered rocks.

Table 6 shows the predicted average estimates of resistance to compression (RC*) from the regression model in all samples.

3 Results and discussion

Regarding the weight losses observed after application of the 70 cycles of both types of artificial ageing, in absolute terms no appreciable changes were observed.

However, upon performing an ANOVA, we found differences between the granites from La Granja and Magullo with respect to Ortigosa del Monte, the latter, which is much more alterable, losing much more material, Fig. 6.

After application of the multivariate Canonical Biplot technique, we obtained a Wilk's lambda of 63.8191 ($p<0.001$), which can be interpreted as though there were differences among the means of the joint measurements of the populations (groups) for all the variables. Regarding the absorption of inertia, the first three axes absorbed 93.989% of the total inertia.

On the first principal plane, plane 1-2 (Fig. 2), which absorbed 76.17% of the inertia, there were clear differences among the three types of varieties of granite before applying the two types of ageing treatment, although no differences were observed for all the variables.

Regarding the L* chromatic coordinate, Ortigosa del Monte (ORT00) and La Granja (GRA00) were lighter than Magullo (MAG00), with no differences between the former two, owing to the size of the crystals and their mineralogical composition. Additionally, the definition of chromaticity (coordinates a* and b*), although with very low values, had higher values on the a* coordinate in the granites from La Granja and there were no differences between the other two. However, on the b* coordinate, the smallest values were obtained for the granites from La Granja and Magullo, and although there were no differences between them, there were differences in comparison with those from Ortigosa del Monte.

Regarding the ultrasound propagation speed, the highest values were obtained for the Magullo granites, followed by those from La Granja and finally those from Ortigosa del Monte, also owing to grain size.

The behaviour of the three types of granite with respect to the number of cycles of each of the ageing treatments was very similar (Figs. 3, 4 and 5). On the same plane, greater effects (distances between markers) were observed in the first 20 cycles as compared with the rest.

On the L* coordinate, it was possible to note a darkening in all the varieties in the first 20 cycles with both ageing treatments, the effect being more noteworthy in T2. From cycle 20 to cycle 70, with T1 a slight degree of darkening persisted, whereas with T2 the samples were seen to become lighter ($p<0.05$) owing to the crystallization of the sodium sulphate decahydrate on the surface of the samples.

Regarding the a* and b* coordinates, in general the definition of the colours increased in parallel with the number of cycles of the two treatments and for all the varieties. In the T1 ageing treatment, fewer significant variations among the cycles were seen as from cycle 20.

With respect to the ultrasound propagation speed (V_x,V_y,V_z), in general with the T1 ageing treatment very few differences were seen in the three varieties. With the T2 ageing treatment, the behaviour was different, since in the first 20 cycles a little increase was observed, followed by a significant decrease in ensuing cycles, these effects being more marked with the Magullo granite This indicates that the synergic action of two processes occurring in the T2 treatment enhances the degree of degradation caused by each of them separately, this type of ageing treatment showing much faster kinetics (Iñigo et al., 2000a). Despite this, the same authors also reported that the freezing/thawing cycles on the silicified granites from Avila led to the opening of microfissures and an increase in the proportion of larger pores in the micropore zone (Iñigo et al., 2000b).

Estimated data resistance to compression by linear regression, Table 6, it follows that produces a decrease in both ageing (T1 and T2). This decrease is much higher in T2 than in T1 in the different stages studied. This is due to the synergistic action of the two processes of T2, which enhance the degradation and increase the kinetics of this process compared to T1 (Iñigo et al., 2000a).

4 Conclusions

Following application of the Canonical Biplot statistical method to the data obtained for all the varieties of granite studied before and after the ageing treatments (T1 and T2), which are as follows the following conclusions may be drawn:

a) The L* chromatic coordinate reveals a darkening in all the varieties of stone in the first 20 cycles of both treatments. After this number of cycles, in the T1 treatment a slight degree of darkening persists (with little difference), while with the T2 treatment the samples become lighter.
b) The a* and b* chromatic coordinates in general point to an increase in the definition of the colours as the number of cycles of both types of ageing treatment increases and for all the varieties.
c) Regarding ultrasound propagation speed, differences were only seen with the T2 treatment. In this case, the behaviour is different because in the first 20 cycles there is a little increase, followed by a significant decrease in the following cycles, these effects being more pronounced in the case of the Magullo granite.

The synergistic action of the combination of two processes (freezing / Thawing and cooling / heating + Salt Crystallization) in the treatment T2 is bigger than both

separately. This is confirmed by the sharp diminution of theoretical data of the resistance to compression through the linear regression model proposed. In addition the kinetics of these processes combined is faster.

Acknowledgements

The authors are grateful for funding from an agreement with the Town Hall of Segovia to perform this work and that from the projects of the National Plan funded by the Ministry of Education and Science (CGL2007-62168BET and FEDER funds) and Ministry of Science and Innovation (MAT2010-20660)]

References

Amaro, I.R., Vicente-Villardón, J.L., Galindo-Villardón, M.P., 2004. ANOVA Biplot para arreglos de tratamientos con dos factores basado en modelos lineales generales multivariantes. Interciencia 29, 26-32.

Amaro, I. R., Vicente Villardón, J.L., Galindo Villardón, M.P., 2008. Contribuciones al MANOVA Biplot: Regiones de Confianza alternativas. <http://rev-inv-ope.univ-paris1.fr/files/29308/IO29308-05.pdf>.

Camuffo, D., 1996. Limits of stone sensitivity to freezing–thawing cycles, in: Vicente, M.A., Delgado Rodrigues, J., Acevedo, J. (ed.), Degradation and conservation of granitic rocks in monuments. EUROPEA COMMISSION, Brussels, Belgium, p. 455–462.

Chen, T.C., Yeung, M.R., Mori, N., 2004. Effect of water saturation on deterioration of welded tuff due to freeze–thaw action. Cold Reg. Sci. Technol. 38, 127–136.

Gabriel, K.R., 1971. The biplot-graphic display of matrices with applications to principal component analysis. Biometrika 58, 453–467.

Gabriel, K.R., 1972. Analysis of meteorological data by means of canonical decomposition and biplots. J. Appl. Meteorol. 11, 1071–1077.

Gabriel, K.R., 1995. Manova biplots for two-way contingency tables, in: Krzanowsky, W. (ed.), Recent Advances in Descriptive Multivariate Analysis. Clarendon Press, Oxford, England, pp. 227–268.

Galindo, M.P., 1986. Una alternativa de representación simultanea: HJ-Biplot. Qüestiió 1, 13-23.

García-Talegón, J., Vicente, M.A., Vicente-Tavera, S., Molina, E., 1998. Assessment of chromatic changes due to artificial ageing and/or conservation treatments of sandstones. Color Res. Appl. 23, 46-51.

García-Talegón, J., Hinojal, R., Iñigo, A.C., Alonso-Gavilán, G., Molina, E., Vicente-Tavera, S., 2006a. El sistema poroso de las areniscas y microconglomerados silicificados de Zamora tras la alteración experimental por hielo/deshielo. Geo-Temas 9, 93-97.

García-Talegón, J., González-Sánchez, M., Iñigo, A.C., Vicente-Tavera, S., Rives, V., 2006b. Microenvironments in the inner and outer parts of the Zamora Catedral, in: Fort, R., Alvarez de Buergo, M., Gomez-Heras, M., Vazquez-Calvo, C. (eds.), Heritage, weathering and conservation. Taylor & Francis/Balkema, Leiden, The Netherlands, pp. 457-461.

Hori, M., Morihiro, H., 1998. Micromechanical analysis on deterioration due to freezing and thawing in porous brittle materials. Int. J. Eng. Sci. 36 (4), 511–522.

Iñigo, A.C., Vicente-Tavera, S., Rives, V., Vicente, M.A., 1997. Colour changes in granitic materials surface by consolidated and/or water repellent treatments. Color Res. Appl. 22, 133-141.

Iñigo, A.C., Rives, V., Vicente, M.A., 2000a. Reproducción en cámara climática de las formas de alteración más frecuentes detectadas en materiales graníticos, en clima de tendencia continental. Mater. Construcc. 50, 57-60.

Iñigo, A.C., Rives, V., Vicente, M.A., 2000b. Weathering and decay of granitic rocks: its relation to their pore network. Mech. Mater. 32, 555-560.

Iñigo, A.C., García-Talegón, J., Trujillano, R., Molina, E., Rives, V., 2003. Evolution and decay processes in the Villamayor and Zamora sandstones, in: Pérez-Rodríguez, J.L. (ed.), Applied Study of Cultural Heritage and Clays. CSIC, Madrid, Spain, pp. 47-57.

Iñigo, A.C., Vicente-Tavera, S., Rives, V., 2004. MANOVA-BIPLOT statistical analysis of the effect of artificial ageing (freezing/thawing) on the colour of treated granite stones. Color Res. Appl. 29, 115-120.

Matsuoka, N., 1990. Mechanisms of rock breakdown by frost action: An experimental approach. Cold Reg. Sci. Technol. 17, 253-270.

Rives, V., García-Talegón, J., 2006. Decay and conservation of building stones on Cultural Heritage monuments. Mater. Sci. Forum 514-516, 560-572.

Sausse, J., Jacquot, E., Fritz, B., Leroy, J., Lespinasse, M., 2001. Evolution of crack permeability during fluidrock interaction: example of the Bre´zouard granite (Vosges, France). Tectonophysics 336, 199–1024.

Sebastián-Pardo, E., Zezza, U., 1998. Colour parameters of calcarenites used in the architectural heritage of the Andalusia (Spain) and Apulia-Basilicata (Italy), in: Fernández-Matrán, M.A. (ed.), Rehabilitación del Patrimonio Arquitectónico y

Edificación. Centro Internacional para la Conservación del Patrimonio, CICOP, Tenerife, Spain, pp. 560-572.

Streckeisen, A., Le Maitre, R.W., 1979. Neues Jahrbuch für Mineralogie. Abhandlungen 136, 169-206.

Takarli, M., Prince, W., Siddique, R., 2008. Damage in granite under heating/cooling cycles and water freeze–thaw condition. Int. J. Rock Mech. Min. 45, 1164–1175.

Tan, X., Chen, W., Yang, J., Cao, J., 2011. Laboratory investigations on the mechanical properties degradation of granite under freeze–thaw cycles. Cold Reg. Sci. Technol. 68, 130–138.

Tiano, P., Pecchioni, E., 1990. Invecchiamento artificiale di materiali lapidei, in: F. Piacenti (ed.), Camera climatiche od ambientali nella ricerca applicata, Firenze, Italy, pp. 37-42.

UNE, 1985. Resistencia a la compresión, granitos ornamentales, 22-175.

Varas, M.J., Vicente-Tavera, S., Molina, E., Vicente-Villardón, J.L., 2005. Role of canonical biplot meted in the study of building stones: an example from Spanish monumental heritage. Environmetrics 16, 1-15.

Vicente, M.A., 1996. Granitic materials and historical monuments: Study of the factors and mechanisms of weathering and application to historical heritage conservation, in: Vicente, M.A., Delgado-Rodrigues, J., Acevedo, J. (eds.), Degradation and conservation of granitic rocks in monuments. EUROPEAN COMMISSION, Brussels, Belgium, pp. 1-44.

Vicente, M.A., Vicente-Tavera, S., 2001. Clay poultices in salt extraction from ornamental stones: A statistical approach. Clay. Clay Miner. 49(3), 227-235.

Vicente-Villardón, J.L., 2012. MULTBIPLOT: Multivariate Analysis using Biplots. <http://biplot.usal.es> (Feb. 6, 2012).

Zezza, F., 2002a. Inland dispersion of marine spray and its effects on monument stone, in: Galán, E., Zezza, F. (eds.), Conservation of Monuments in the Mediterranean Basin. Swets & Zeitlinger BV, Lisse, The Netherlands, pp. 23-39.

Zezza, F., 2002b. Non-destructive technique for the assessment of the deterioration processes of prehistoric rock art in karstic caves: the paleolithic paintings of Altamira (Spain), in: Galán, E., Zezza, F. (eds.), Conservation of Monuments in the Mediterranean Basin. Swets & Zeitlinger BV, Lisse, The Netherlands, pp. 377-388.

Figure captions

Fig. 1. Q' ANOR' chemical classification of the granite varieties studied.

Fig. 2. Simultaneous plot on plane 1-2 obtained after application of the Canonical Biplot method.

Fig. 3. Plot of the 1-2 plane obtained after application of the Canonical Biplot method of the La Granja granite variety

Fig. 4. Plot of the 1-2 plane obtained after application of the Canonical Biplot method of the Ortigosa del Monte granite variety.

Fig. 5. Plot of the 1-2 plane obtained after application of the Canonical Biplot method of the Magullo granite variety.

Fig. 6. Plot of the Nº cycles/type of sample interaction for the weight loss variable

Table(s)

Table 1: Mineralogical composition of the different granites studied.

Sample	Q	Fk	Pl	I/M
Ortigosa del Monte	xxx	xx	xx	xx
La Granja	xxx	xxx	xxx	x
Magullo	xxx	xx	xx	xx

Q: quartz, Fk: potassium feldspar, Pl: plagioclase, I/M: micas

xxx: dominant, xx: abundant, x:present

Table(s)

Table 2: Chemical composition of the major elements of each of the granite varieties studied.

Sample	SiO_2[a]	Al_2O_3[a]	TiO_2[a]	Fe_2O_3[a]	MnO[a]	MgO[a]	CaO[a]	Na_2O[a]	K_2O[a]	P_2O_5[a]	V.M.[a]
Ortigosa del Monte	71.33	14.14	0,24	1.99	0.03	0.3	1.19	3.47	5.32	0.15	1.34
La Granja	72.73	14.16	0,27	1.85	0.03	0.18	1.54	3.30	3.98	0.11	1.35
Magullo	69.64	15.55	0,47	2.9	0.06	0.73	2.5	3.58	3.19	0.13	0.75

[a]: % oxides of major elements, V.M.: Volatile material

Table(s)

Table 3: Average data of different varieties of granite for each of the variables studied (colour coordinates and the ultrasound propagation speed)

	Vx		Vy		Vz		L*		a*		b*	
Sample	Mean	S.E.	Mean	S.E.	Mean	S.E.	Mean	S.E.	Mean	S.E.	Mean	S.E.
GRA00	3084	65	3430	52	3198	47	71.2	0.1	-0.68	0.03	1.32	0.74
GT120	3069	106	3176	61	3037	73	68.9	0.3	-0.14	0.04	4.02	0.11
GT140	2575	76	3103	56	2846	77	69.9	0.3	0.12	0.04	2.73	0.09
GT160	2562	65	3070	66	2731	73	67.8	0.3	0.04	0.03	5.05	0.10
GT170	2666	74	3137	71	2841	64	67.3	0.3	0.02	0.03	5.51	0.11
GT220	3034	89	3268	43	3102	50	66.7	0.3	0.14	0.05	1.96	0.18
GT240	2632	51	2861	53	2733	53	65.9	0.3	-0.22	0.04	2.88	0.11
GT260	2410	48	2649	64	2508	53	65.0	0.3	-0.14	0.05	3.43	0.10
GT270	1977	38	2268	40	2054	52	66.0	0.3	-0.06	0.05	3.31	0.10
MAG00	3379	40	3626	33	3389	36	66.2	0.1	-0.58	0.01	-0.64	0.05
MT120	3310	29	3520	35	3285	38	63.5	0.2	-0.05	0.02	2.83	0.10
MT140	3229	51	3306	35	3151	15	64.4	0.2	0.05	0.02	1.61	0.08
MT160	3184	52	3204	39	3077	29	62.6	0.2	0.00	0.02	3.25	0.29
MT170	3198	33	3338	21	3186	25	62.1	0.2	0.01	0.03	4.19	0.11
MT220	3342	28	3519	32	3418	39	61.0	0.2	0.19	0.03	1.41	0.06
MT240	3169	47	3030	45	3262	44	61.1	0.2	-0.01	0.03	2.15	0.07
MT260	2564	29	2450	44	2349	38	62.4	0.2	0.08	0.03	2.33	0.18
MT270	1741	27	1770	39	1823	30	63.0	0.2	0.17	0.02	2.37	0.08
OTE00	2423	24	2428	28	2370	27	72.6	0.2	-0.24	0.01	1.47	0.04
OT120	2294	25	2185	38	2156	41	70.6	0.3	0.59	0.02	3.36	0.05
OT140	2322	26	2293	48	2136	43	69.5	0.3	0.27	0.02	4.68	0.08
OT160	2290	17	2115	43	2088	50	68.4	0.3	0.41	0.02	5.69	0.08
OT170	2320	19	2190	51	2103	42	67.9	0.3	0.39	0.02	6.18	0.08
OT220	2493	15	2471	47	2429	36	69.5	0.5	0.83	0.06	2.47	0.13
OT240	2247	26	2293	31	2325	40	67.7	0.3	0.45	0.03	3.38	0.12
OT260	1826	30	1879	19	1891	30	67.3	0.3	0.51	0.03	4.14	0.10
OT270	1532	32	1496	30	1570	37	67.0	0.3	0.55	0.02	4.12	0.13

x
Vx, Vy and Vz = Ultrasound propagation speed (m/s), S.E.: Standard Error

Table(s)

Table 4: Resistance to compression and ultrasound propagation speed in altered or no granites.

RC	V	Altered	Granite
1035	4198	No	Avila
670	3933	No	Avila
1028	4720	No	Braga
1072	4689	No	Braga
989	4707	No	Braga
1046	4678	No	Braga
581	4626	No	Braga
881	4656	No	Braga
1362	4703	No	Braga
1386	4623	No	Braga
1138	4043	No	Porto
1243	3834	No	Porto
690	3145	No	Porto
1227	3945	No	Porto
281	2201	Yes	Avila
485	2587	Yes	Avila
428	2781	Yes	Avila
830	3695	Yes	Braga
896	3531	Yes	Braga
828	3416	Yes	Braga
906	3459	Yes	Braga
352	2723	Yes	Braga
741	3697	Yes	Braga
617	4050	Yes	Braga
630	2832	Yes	Porto
631	3209	Yes	Porto
661	2886	Yes	Porto
582	2576	Yes	Porto

RC= Resistance to compression (Kg/m^2), V= ultrasonic propagation speed (m/s)

Table(s)

Table 5: Results of linear regression model.

R	R Squared	Adjusted R Squared	Standard Error
0.765	0.586	0.553	198.35194

ANOVA

Source	Sum of Squares	DF	Mean Square	F-value	p-value
Regression	1391003.519	2	695501.760	17.678	0.000
Residual	983587.338	25	39343.494		
Total	2374590.857	27			

MODEL COEFICIENTS

Model	Non standard Coefficients		Standardized Coefficients	t	p-value
	β	Standard Error			
Intercept	146.983	333.902		0.440	0.664
V	0.203	0.076	0.542	2.663	0.013
Altered	-153.971	118.565	-0.264	-1.299	0.206

Table(s)

Table 6: Average estimates of resistance to compression (RC*) from the regression model.

Samples	V	Ageing	RC*
GRA00	3237	0	804
GT120	3094	1	621
GT140	2841	1	570
GT160	2788	1	559
GT170	2881	1	578
GT220	3135	1	629
GT240	2742	1	550
GT260	2522	1	505
GT270	2100	1	419
MAG00	3465	0	850
MT120	3372	1	677
MT140	3229	1	648
MT160	3155	1	633
MT170	3241	1	651
MT220	3426	1	689
MT240	3154	1	633
MT260	2454	1	491
MT270	1778	1	354
OTE00	2407	0	636
OT120	2212	1	442
OT140	2250	1	450
OT160	2164	1	432
OT170	2204	1	440
OT220	2464	1	493
OT240	2288	1	458
OT260	1865	1	372
OT270	1533	1	304

V= Average of ultrasound propagation speed (m/s),
RC*= Average estimates of resistance to compression (Kg/m^2)

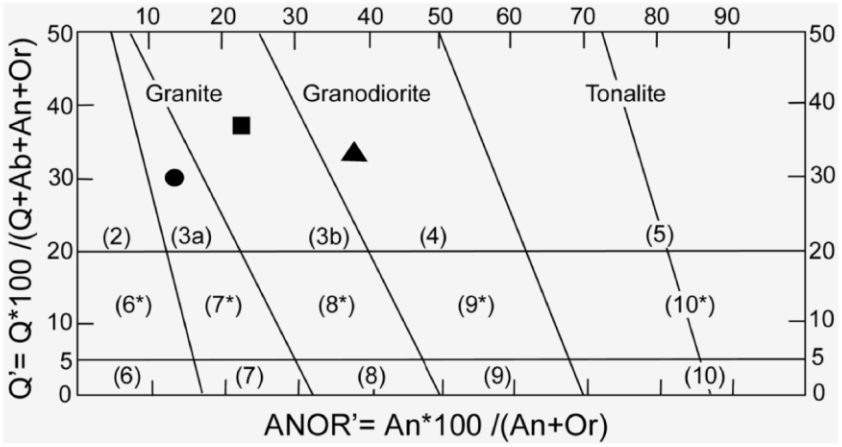

Q: quartz; Ab: albite; An: anorthite; Or: orthoclase

● Ortigosa del Monte ■ La Granja ▲ Magullo

2 Alkali feldspar granite

3 Granite
a) Syenogranite (=calcalkaline g.)
b) Monzogranite (adamellite)

4 Granodiorite

5 Tonalite

6* Alkali feldspar quartz-syenite

6 Alkali feldspar syenite

7* Quartz-syenite

7 Syenite

8* Quartz-monzonite

8 Monzonite

9* Quartz monzogabbro
Quartz monzodiorite

9 Monzodiorite
Monzogabbro

10* Quartz-diorite
Quartz-gabbro
Quartz-anorthosite

10 Diorite (M>10, An<50)
Gabbro (M>10, An>50)
Anorthosite (M<10)

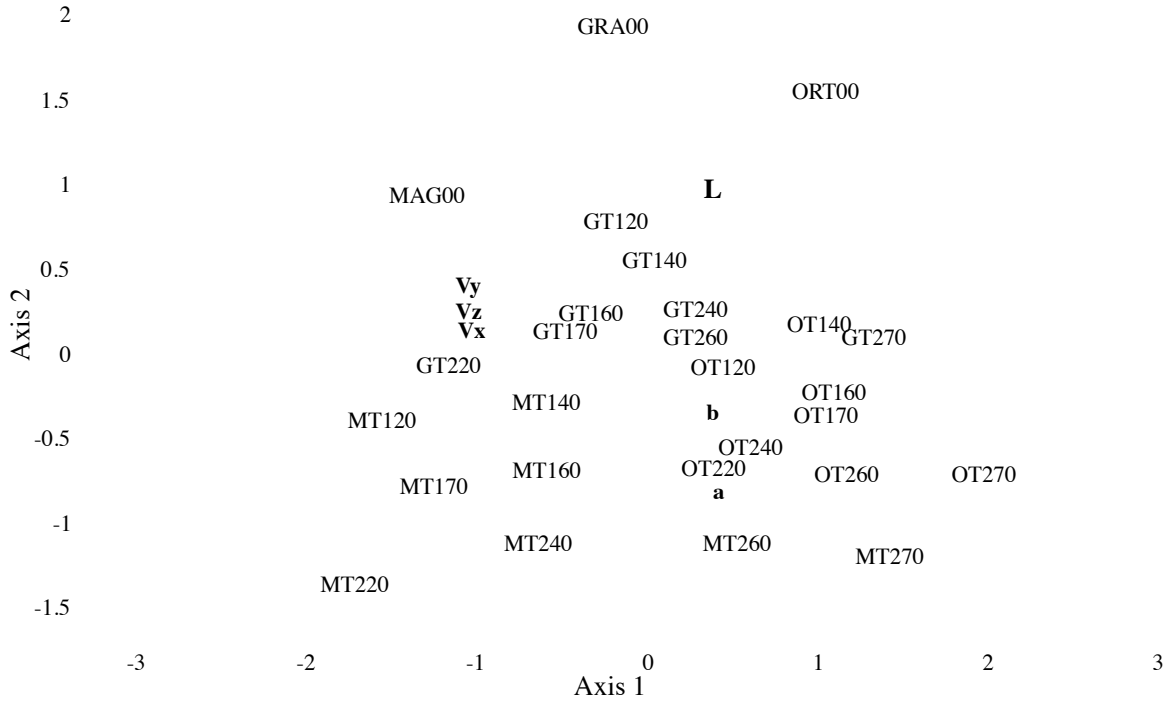
2
1.5
1
0.5
0
-0.5
-1
-1.5
Axis 2
-3
-2
-1
0
1
2
3
Axis 1
GRA00
ORT00
MAG00
L
GT120
GT140
Vy
Vz
Vx
GT160
GT170
GT240
GT260
OT140
GT270
GT220
OT120
OT160
MT140
MT120
b
OT170
OT240
MT160
OT220
OT260
OT270
MT170
a
MT240
MT260
MT270
MT220

Figure(s)

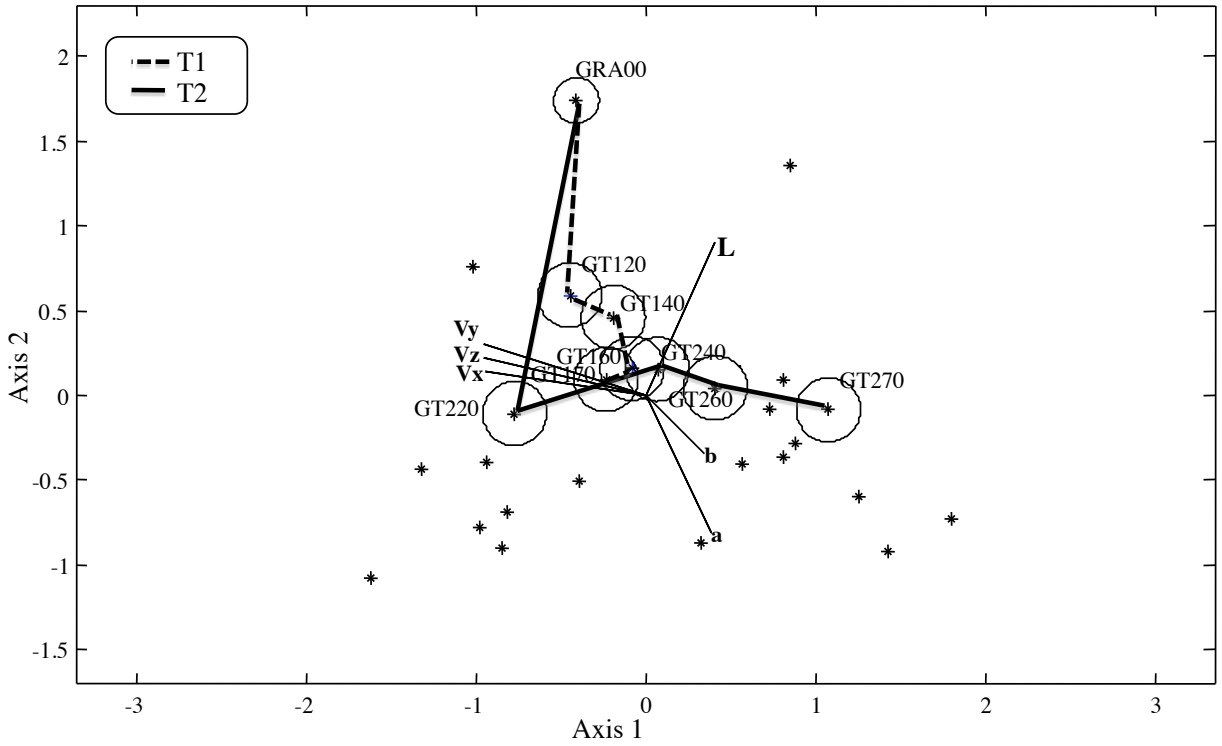
T1
T2
GRA00
L
GT120
GT140
Vy
Vz
Vx
GT160
GT240
GT270
GT220
GT260
b
a
Axis 2
Axis 1
2
1.5
1
0.5
0
-0.5
-1
-1.5
-3
-2
-1
0
1
2
3

Figure(s)

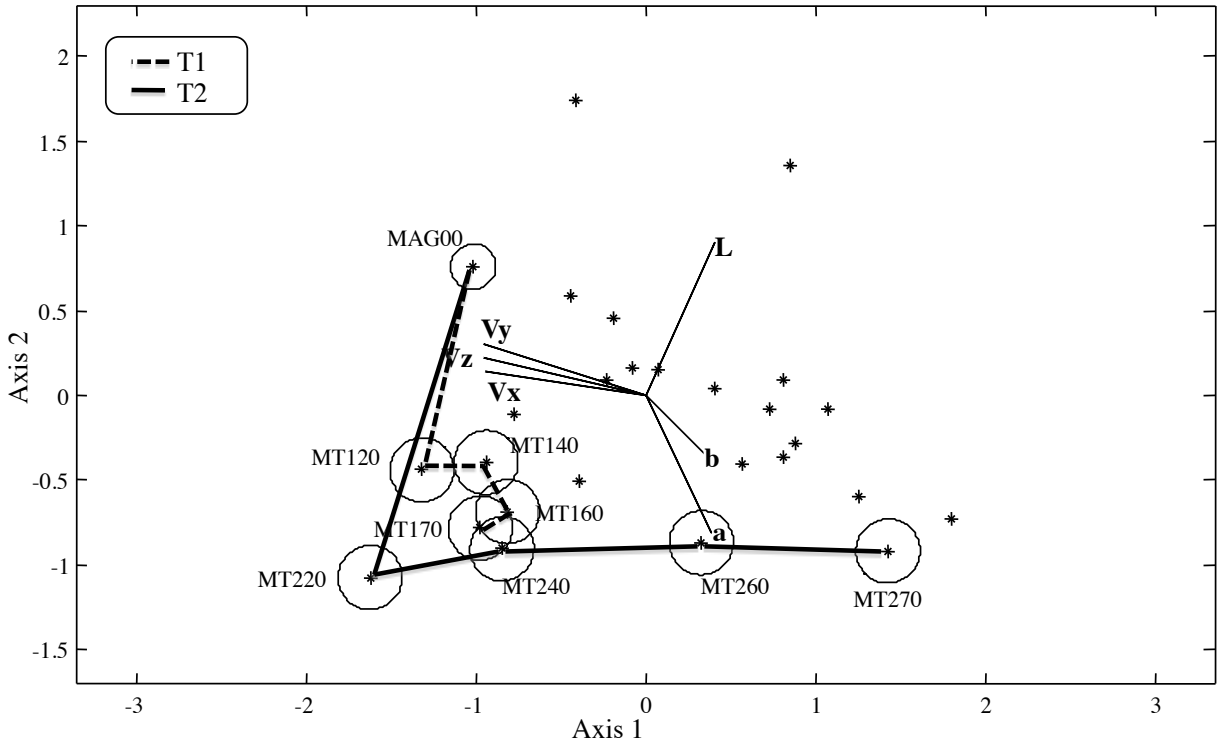
T1
T2
MAG00
L
Vy
Vz
Vx
MT120
MT140
b
MT160
MT170
a
MT220
MT240
MT260
MT270
Axis 2
Axis 1
2
1.5
1
0.5
0
-0.5
-1
-1.5
-3
-2
-1
0
1
2
3

Figure(s)

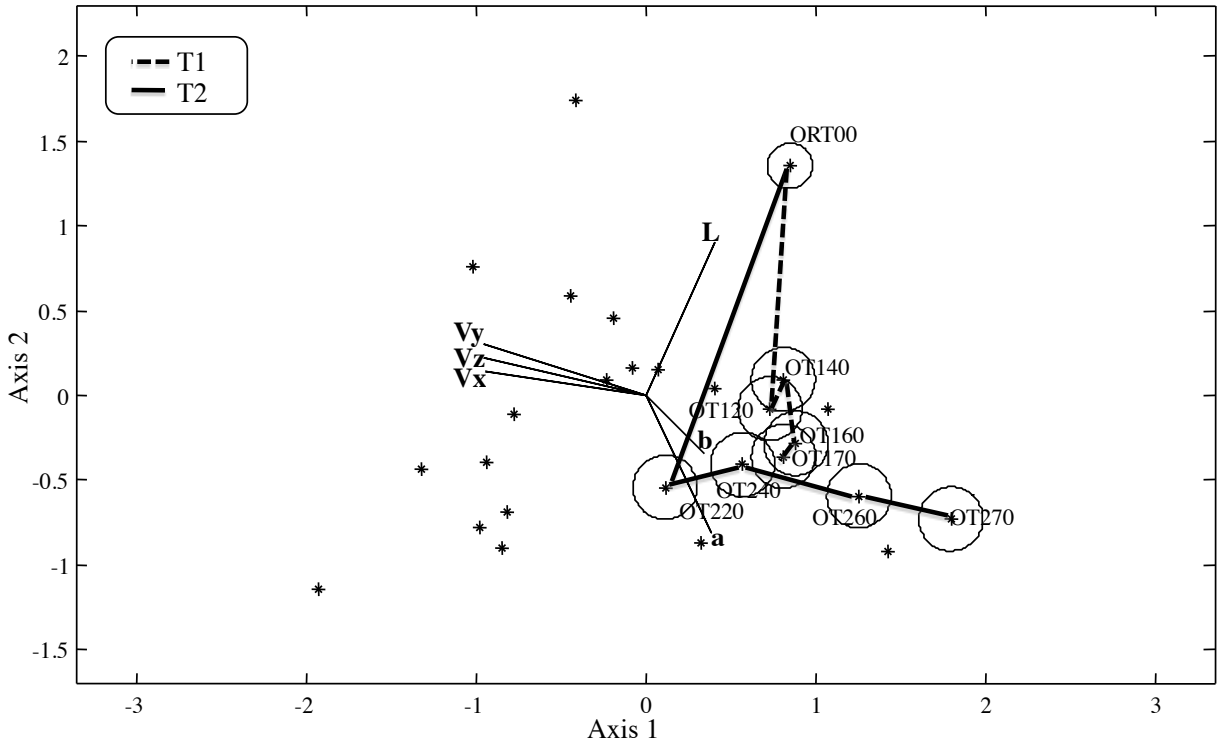
T1
T2
ORT00
L
Vy
Vz
Vx
OT140
OT120
b
OT160
OT170
OT240
OT220
a
OT260
OT270
Axis 2
Axis 1
2
1.5
1
0.5
0
-0.5
-1
-1.5
-3
-2
-1
0
1
2
3

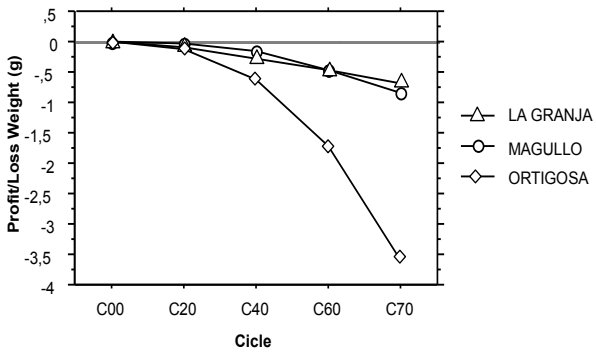
,5
0
-,5
-1
-1,5
-2
-2,5
-3
-3,5
-4
Profit/Loss Weight (g)
C00
C20
C40
C60
C70
Cicle
LA GRANJA
MAGULLO
ORTIGOSA